Joint International Topical Meeting on Mathematics & Computation and Supercomputing in Nuclear Applications (M&C + SNA 2007)
Monterey, California, April 15-19, 2007, on CD-ROM, American Nuclear Society, La Grange Park, IL (2007)

A MONTE CARLO METHOD FOR CALCULATING INITIATION PROBABILITY

Gregory Greenman, Richard Procassini and Christopher Clouse

Lawrence Livermore National Laboratory
Mail Stop L-95, P.O. Box 808
Livermore, CA 94551
United States of America

greenman1@llnl.gov, spike@llnl.gov, clouse1@llnl.gov

ABSTRACT

A Monte Carlo method for calculating the probability of initiating a self-sustaining neutron chain reaction has been developed. In contrast to deterministic codes which solve a non-linear, adjoint form of the Boltzmann equation to calculate initiation probability, this new method solves the forward (standard) form of the equation using a modified source calculation technique. Results from this new method are compared with results obtained from several deterministic codes for a suite of historical test problems. The level of agreement between these code predictions is quite good, considering the use of different numerical techniques and nuclear data. A set of modifications to the historical test problems has also been developed which reduces the impact of neutron source ambiguities on the calculated probabilities.

Key Words:probability of initiation, self-sustaining chain reaction, Monte Carlo methods

1. INTRODUCTION

The criticality of fissile (neutron multiplying) systems can described by either of two eigenvalues. These are (a) the effective neutron multiplication factor $k_{eff} \equiv N^{g+1}/N^{g}$, which is defined as the average number of neutrons (N) created by fission in the *succeeding* neutron generation per neutron in the *current* generation, and (b) the logarithmic rate of change of the neutron population $\alpha \equiv (1/N)(dN/dt)$. For many fissile systems, the use of either k_{eff} or α provides an adequate representation of the change in neutron population with time. However, there are systems for which these *static* eigenvalues do not adequately describe the probability that the neutron population will grow ($k_{eff} > 1$ or $\alpha > 0$), shrink ($k_{eff} < 1$ or $\alpha < 0$) or remaining constant ($k_{eff} = 1$ or $\alpha = 0$) over time.

For example, a pulsed reactor may be driven super-prompt critical ($k_{eff} > 1$ and $\alpha > 0$) for a short period of time by the rapid mechanical insertion of a slug of fissile material into the core. If the neutron generation time is comparable to the period over which the fissile mass is varying, then the assumption of a static system, which is inherent in the definition of k_{eff}, is no longer valid. In this case, one can determine the *probability* that this dynamic system will become critical. The key to such a *initiation probability* method is the ability to calculate the probability that a single neutron will lead to a divergent, or self-sustaining, chain reaction in the multiplying medium.

The classic method for obtaining the initiation probability of a fissile system is the solution the Bell equation [1], which is an adjoint form of the Boltzmann transport equation with a modified fission term. However, other methods can also be employed for this purpose. We have developed a non-adjoint, Monte Carlo technique for calculating the initiation probability. This method is based upon a solution of the forward form Boltzmann transport equation. This method has recently been implemented in the **Mercury** Monte Carlo particle transport code [2], [3]. The method can be used in conjunction with the wide variety of tracking options supported in the code, for both mesh-based and combinatorial problem geometries. In addition, the method has been adopted to support both spatial (domain decomposition) and particle (domain replication) parallelism.

The Monte Carlo algorithm for calculating initiation probability will be described in the next section. This will be followed in Section 3 by a comparison of the results obtained from **Mercury** with results obtained from deterministic codes for a series of historical test problems. This comparison has prompted the development of another suite of test problems with a less-ambiguous definition of the neutron source, which is described in the same section. The paper concludes with a summary and plan for future work on this algorithm.

2. INITIATION PROBABILITY VIA THE MONTE CARLO METHOD

Our goal is to calculate the probability that a fissile, or neutron multiplying, system will initiate a self-sustaining neutron chain reaction. Consider a critical or super-critical system in the absence of any neutrons. This system will remain in a stationary state until a stray neutron happens by and induces a fission event, which commences a neutron chain reaction. The probability that a given source of neutrons will initiate a self-sustaining neutron chain is given by

$$P = 1 - e^{-\int\int\int S(r,E,t)\,p(r,E,t)\,dr\,dE\,dt} \tag{1}$$

where $S(r,E,t)$ is the space-, energy-and time-dependent source function, and $p(r,E,t)$ is the space-, energy-and time-dependent probability that a *single* neutron will produce a divergent (persistent) fission chain.

A standard approach for calculating $p(r,E,t)$ is to deterministically solve the equation derived by Bell [1]. This integro-differential equation is similar to the α adjoint form of the Boltzmann transport equation, but which includes a non-linear fission multiplicity term. This method has been implemented in several discrete ordinates (S_N) codes, including the **Partisn** code from the Los Alamos National Laboratory [4], and the **Ardra** [5] and **Amtran** [6] codes from the Lawrence Livermore National Laboratory. These codes use an non-linear iteration scheme (outside of the loops which solve the linear adjoint transport equation) to model the possibility that a variety of numbers of neutrons are emitted by a single fission event.

An alternative method has been implemented in the **Mercury** Monte Carlo code. This technique is based upon an analog solution of the forward (standard) form of the Boltzmann transport equation. In contrast to *criticality* methods for calculating the k_{eff} or α eigenvalues of the system, this new method is a modification of a time-dependent *source* calculation. To start the initiation probability calculation, a collection of source neutrons $S(r,E,t)$ is injected into the system. These represent the progenitors of a series of neutron families or chains, which along with their progeny, are tracked forward in time.

In addition to defining the characteristics of the neutron source distribution, the user must provide a few additional parameters to the model. These include (a) the number of progeny neutrons per progenitor which are required to define a divergent family/chain (successful_chain_threshold), (b) the maximum age for which any chain is integrated (tracked) forward in time (max_age), and (c) the number of sub-intervals within the maximum chain age (num_substeps). At each sub-interval, the method checks the number of progeny that have been accumulated in each family, comparing this to the input threshold value to determine whether the chain has become self sustaining. The number of chains that have exceeded the divergence threshold is also carried forward in time. The single-neutron probability of initiation is defined as the ratio of the number of divergent chains to the initial number of chains

$$p^k(r, E, t) \equiv \frac{C_d^k}{C_i} \tag{2}$$

where C_i is the number of chains (progenitor neutrons) created by the user defined source and C_d^k is the number of divergent chains accumulated through sub-interval k.

The maximum age parameter is used to limit the time over which neutron chains are integrated (tallied), based upon the characteristics of the dynamic system. For example, consider a pulsed reactor where the fissile slug is resident in the core for a short time interval. In this case, it would not be accurate to compute initiation probability for time periods which are greater than the slug residence time. The ability to limit the time integration interval in this new method is one of its strengths relative to the available deterministic methods. Each of the aforementioned S_N codes compute the initiation probability via solution of a *static* adjoint form of the Boltzmann equation, which implies an infinite period of time over which the neutron chains are integrated. As a result, these codes will tend to *overestimate* the pulsed reactor probability of initiation.

Although this new method has the advantage of evolving the neutron chains for less than an infinite time period, one may be concerned that the maximum age parameter may not have been set large enough to guarantee that the initiation probability has reached an asymptotic state. However, the use of sub-intervals in this method permits the user to monitor the asymptotic approach of the probability towards convergence. If convergence has not been achieved for a given maximum age, the user may rerun the simulation with a longer integration time. The other user defined parameter that could lead to a false sense of convergence is the threshold count for a chain to be considered divergent. In general, the user should run several simulations for a given type of problem over which this threshold is varied to ensure that the reported probabilities are indeed convergent. Experience with this method has shown that the divergence threshold can be set to $\mathcal{O}(10000)$ for most near-critical systems $(k_{eff} \approx 1)$, while most super-critical systems $(\alpha > 0)$ can safely achieve convergence in as little as $\mathcal{O}(1000)$ progeny per chain. Finally, it should be noted that the other free parameter in this model, the initial number of chains C_i created in the user defined source, only affects the level accuracy at which the initiation probability can be quoted. For instance, $C_i = 100$ initial chains will produce accurate probability estimates at the 1% error level.

This method requires a mechanism by which any neutron being tracked can be efficiently associated with its family and the source progenitor neutron of that family. The particle identifier attribute in **Mercury** has been used for this purpose. The code's default mode of operation has

each particle being assigned its own unique identifier. When run in "criticality probability" mode, each particle produced within a family is assigned the identifier of its progenitor, and only the original sourced (progenitor) neutrons are assigned unique identifiers. At the end of each sub-interval, a census of family members is taken by counting the number of particles associated with each unique identifier. A data structure holds the census count of each of the families/ chains. Once the number of neutrons in a given family has exceeded the user defined threshold, the chain member count is set to '-1', signifying that the chain has become divergent. As each of the neutron families achieves a self-sustaining level, their progeny are deleted from the calculation, in the interest of computational efficiency.

While the process of determining the number of neutrons in each chain is straightforward for serial calculations, it is somewhat more complicated for parallel computations. The complexity arises from the use of spatial domain decomposition (spatial parallelism) techniques, and is not encountered for domain replication forms of (particle) parallelism. In the latter, the particle work load is distributed across multiple processors, each of which is responsible for the entire problem geometry and where each chain can be assigned to a single processor. In the former, any particle in a chain can track to an inter-processor domain boundary, and be communicated to a different processor before continuing its track. As a result, a given particle chain could evolve to inhabit several domains/processors. In order to determine whether any chain has become divergent, a redundant version of the census data structure exists on each processor. A local census of family members is performed on every processor, and the results of that partial census undergo a summed reduction across processors to arrive at the global count, which is then stored on each processor.

3. TEST PROBLEM RESULTS

A suite of test problems were developed by researchers at LANL and LLNL in the late 1970s [7] which may be used to validate probability of initiation methods. These are a series of bare homogeneous spheres that are comprised of either highly enriched uranium (oralloy) or δ -phase plutonium. The density and radius of the spheres were varied to give a series of problems at different values of ρr, or "optical depth". The description of these "legacy" test problems is provided in Tables 1 and 2. These various configurations have been used to compare code predictions of both the α eigenvalue and single-particle initiation probability $p(r, E, t)$ for a specified neutron source distribution $S(r, E, t)$ of unity amplitude. The rationale for choosing test spheres of varying ρr is that different values of the density and radius may be chosen to conserve ρr, and the probability $p(r, E, t)$ should be invariant to such a change, while the α eigenvalue is subject to change.

Predictions for both the α eigenvalue and the probability $p(r, E, t)$ for these test problems have been obtained from the **Mercury** Monte Carlo code and the **Amtran**, **Ardra** and **Partisn** deterministic (S_N) codes. The calculations with the LLNL codes (**Mercury**, **Amtran** and **Ardra**) used the ENDL-99 [8] evaluated nuclear data base, while the **Partisn** calculation used the LANL MENDF-6 [9] multi-group version of the ENDF/B-VI nuclear data base. The **Mercury** run used a continuous energy representation of the cross sections, while the S_N codes used with 175-group (**Amtran** and **Ardra**) or 30-group (**Partisn**) multi-group cross sections. The other S_N run parameters used in **Amtran** / **Ardra** / **Partisn** include angular quadrature of S_{24} / S_{40} /

Table 1. Highly-Enriched-Uranium Bare Sphere Test Problem Description

ρr	ρ [g/cm^3]	r [cm]
165	19.0	8.6842
195	24.4	7.9918
225	30.3	7.4257
255	36.6	6.9672
285	43.2	6.5972
315	50.2	6.2749

Isotopic Atom Fractions: $^{235}U \rightarrow 9.38x10^{-1}$, $^{238}U \rightarrow 6.20x10^{-2}$

Table 2. δ -Phase Plutonium Bare Sphere Test Problem Description

ρr	ρ [g/cm^3]	r [cm]
100	15.7	6.3694
120	20.6	5.8252
140	26.0	5.3846
160	31.8	5.0314
180	37.9	4.7493

Isotopic Atom Fractions: Ga $\rightarrow 2.6030x10^{-2}$, $^{239}Pu \rightarrow 9.3105x10^{-1}$, $^{240}Pu \rightarrow 5.6440x10^{-2}$, $^{241}Pu \rightarrow 4.48x10^{-3}$

S_{16}, Legendre expansion of P_2 / P_2 / P_4, and 8 / 8 / 5 fission multiplicity terms. The parameters used in **Mercury** include $C_i = 10000$ fission chains/families, successful_chain_ threshold = 1000 progeny, and a maximum integration time of max_age = 1 μ sec comprised of num_ substeps = 1000 sub-intervals. Each of these runs employed an isotropic, spherical source of radius $r_{source} = r_{sphere}$, with a fission-spectrum energy dependence that was obtained from the tabulated ENDL-99 data base (LLNL codes) or an analytic Watt spectrum (**Partisn**). Finally, the fission neutron multiplicity data used in each of the codes is based upon the analytic model developed by Terrell [10], which assumes that the number of neutrons emitted by a fission event $f(\nu)$ can be described by a truncated Gaussian distribution.

The α eigenvalues and the probabilities $p(r, E, t)$ obtained from these codes is plotted in Figures 1 and 2 for the uranium and plutonium bare-sphere test problems, respectively. The Mercury results are also tabulated in Tables 3 and 4. The general trend for both the α eigenvalue and the probability of initiation is to increase with increasing ρr. However, Figures 1 and 2 clearly show that α eigenvalue increases with a greater-than-linear slope, while $p(r, E, t)$ increases with a less-than-linear slope. The level of agreement between the various codes is quite good. The α eigenvalues predicted by **Mercury** and **Partisn** agree to within 5.2% at low α values, and to within 1.8% at high α values. When one considers that these results were ob-

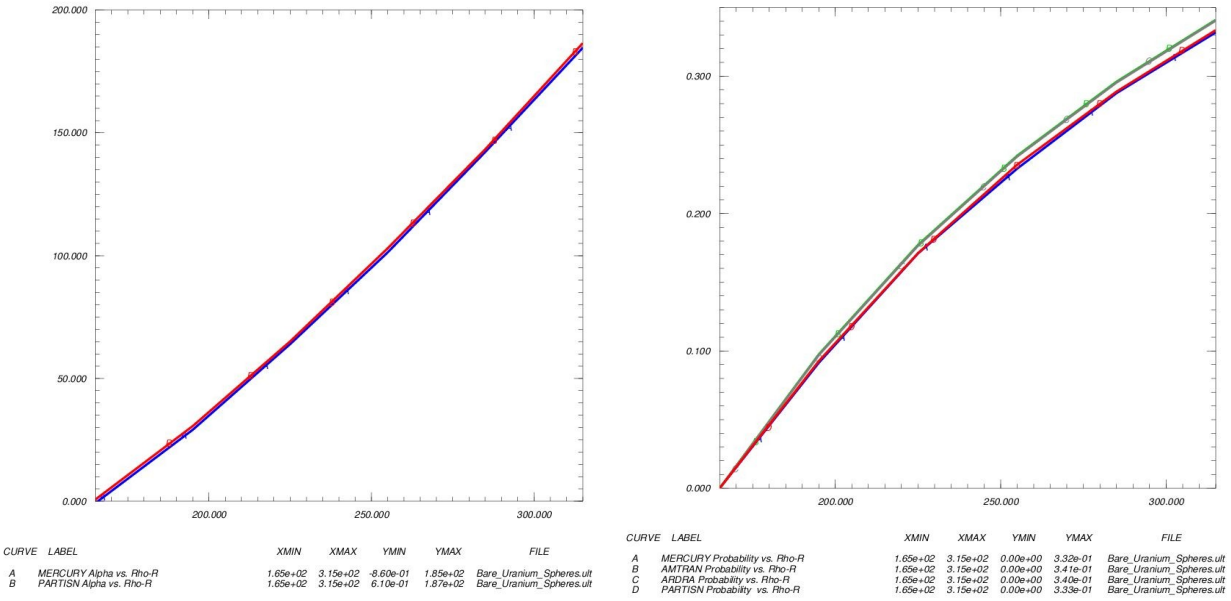

(a) (b)

Figure 1. The (a) predicted α eigenvalues and (b) single-particle initiation probabilities for the bare uranium sphere test problems as obtained from several codes. The results from the **Mercury** Monte Carlo code are shown in blue.

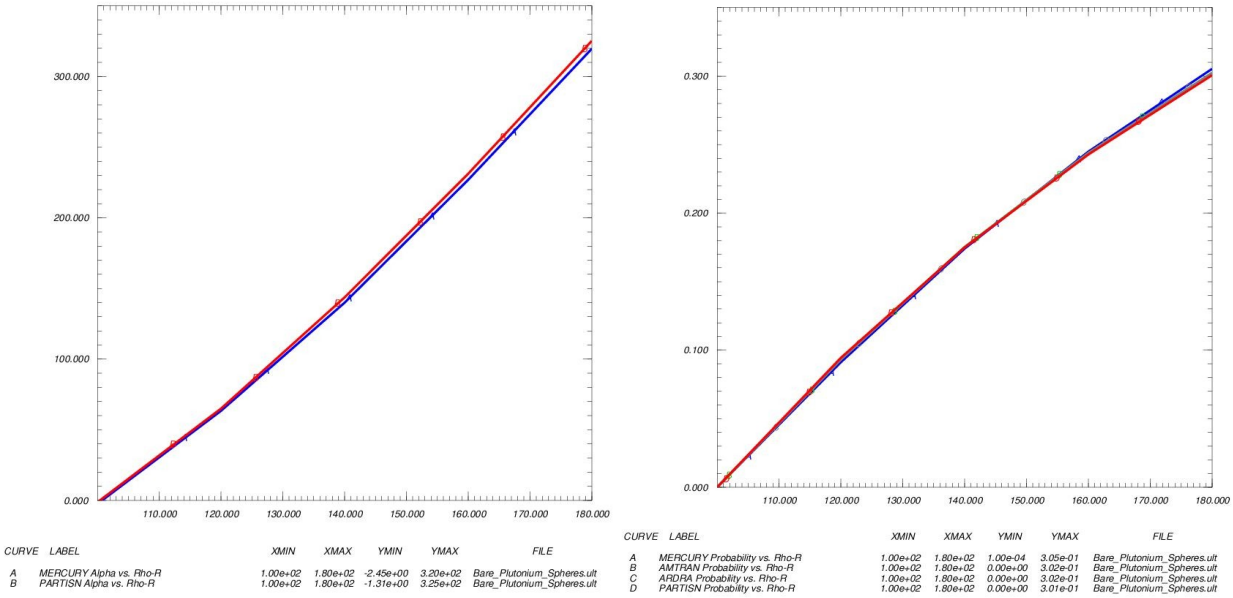

(a) (b)

Figure 2. The (a) predicted α eigenvalues and (b) single-particle initiation probabilities for the bare plutonium sphere test problems as obtained from several codes. The results from the **Mercury** Monte Carlo code are shown in blue.

Table 3. Highly-Enriched-Uranium Bare Sphere Test Problem Results (Mercury)

ρr	α **[gen/ μ sec]**	p **[%]**
165	-0.9	0.00
195	29.1	9.14
225	64.0	17.10
255	101.3	23.28
285	142.2	28.77
315	184.6	33.19

Table 4. δ -Phase Plutonium Bare Sphere Test Problem Results (Mercury)

ρr	α **[gen/ μ sec]**	p **[%]**
100	-2.5	0.01
120	63.4	9.12
140	140.0	17.40
160	226.9	24.49
180	319.6	30.53

tained from codes using different transport algorithms and nuclear data, these differences are quite acceptable. The predicted initiation probabilities $p(r, E, t)$ agree to within 2.7% for the uranium spheres (maximum error at $\rho r = 315$ g/cm^2), and to within 1.5% for the plutonium spheres (maximum error also at $\rho r = 315$ g/cm^2). It should be pointed out that the level of agreement illustrated in Figures 1b and 2b is much better than was observed for the predictions of "legacy" codes (~13 – 17%) that were developed at LANL and LLNL in the 1970s and 1980s [7].

The single-particle initiation probability can be rather sensitive to the spatial and energy distribution of the neutrons emitted by the source $S(r, E, t)$. For example, by changing the radius of the source in the $\rho r = 255$ g/cm^2 uranium sphere calculation from $r_{source} = r_{sphere} = 6.9672$ cm to $r_{source} = 1$ cm, the initiation probability changes from $p = 23.28$ % to $p = 43.92$ %. In addition, there is the possibility that small differences in the energy dependence of the fission spectrum between the evaluated nuclear data bases and the Watt analytic spectrum could have an impact on the predictions of $p(r, E, t)$. Therefore, we propose a simplified set of test problems which are extensions of those defined above. The intent of these new test problems is to eliminate ambiguity in the definition of the neutron particle source. These new test problems utilize a source with (a) a spatial singularity $r_{source} = 0$ cm (or as spatially-compact a source as the transport code can accommodate), with (b) a series of monoenergetic emissions energies $E_{source} = 10$, $1, 10^{-1}, 10^{-2}, 10^{-3}, 10^{-4}, 10^{-5}, 10^{-6}$ or 10^{-7} MeV, and (c) isotropic angular emission.

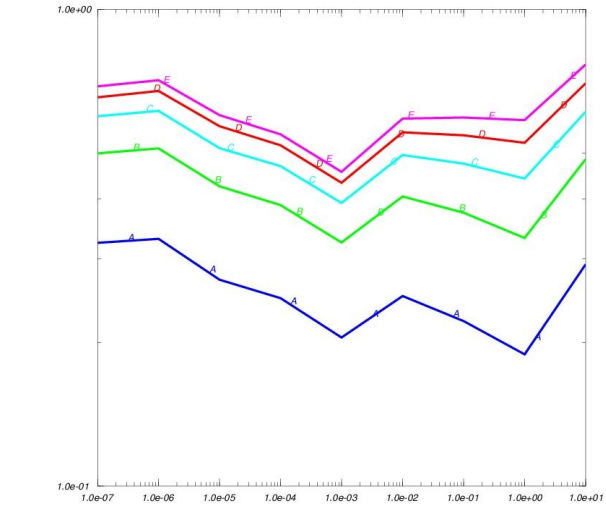

CURVE	LABEL	XMIN	XMAX	YMIN	YMAX	FILE
A	Probability vs Energy (Rho-R = 195)	1.00e-07	1.00e+01	1.89e-01	3.30e-01	Bare_Uranium_Spheres.ult
B	Probability vs Energy (Rho-R = 225)	1.00e-07	1.00e+01	3.25e-01	5.11e-01	Bare_Uranium_Spheres.ult
C	Probability vs Energy (Rho-R = 255)	1.00e-07	1.00e+01	3.93e-01	6.13e-01	Bare_Uranium_Spheres.ult
D	Probability vs Energy (Rho-R = 285)	1.00e-07	1.00e+01	4.33e-01	7.00e-01	Bare_Uranium_Spheres.ult
E	Probability vs Energy (Rho-R = 315)	1.00e-07	1.00e+01	4.57e-01	7.66e-01	Bare_Uranium_Spheres.ult

(a)

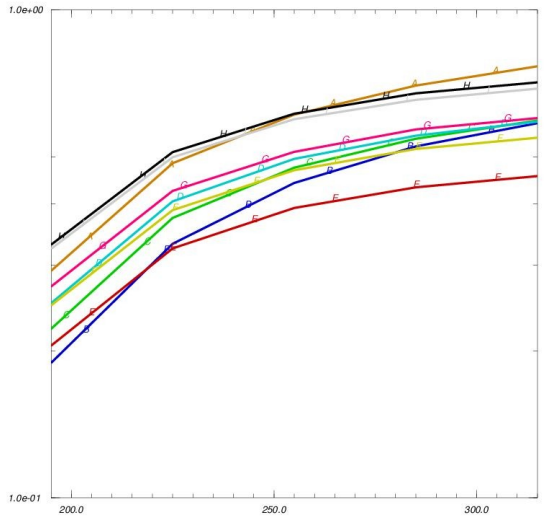

CURVE	LABEL	XMIN	XMAX	YMIN	YMAX	FILE
A	Probability vs Rho-R (Energy = 10^+1)	1.95e+02	3.15e+02	2.92e-01	7.66e-01	Bare_Uranium_Spheres.ult
B	Probability vs Rho-R (Energy = 10^+0)	1.95e+02	3.15e+02	1.89e-01	5.86e-01	Bare_Uranium_Spheres.ult
C	Probability vs Rho-R (Energy = 10^-1)	1.95e+02	3.15e+02	2.22e-01	5.93e-01	Bare_Uranium_Spheres.ult
D	Probability vs Rho-R (Energy = 10^-2)	1.95e+02	3.15e+02	2.50e-01	5.90e-01	Bare_Uranium_Spheres.ult
E	Probability vs Rho-R (Energy = 10^-3)	1.95e+02	3.15e+02	2.05e-01	4.57e-01	Bare_Uranium_Spheres.ult
F	Probability vs Rho-R (Energy = 10^-4)	1.95e+02	3.15e+02	2.48e-01	5.47e-01	Bare_Uranium_Spheres.ult
G	Probability vs Rho-R (Energy = 10^-5)	1.95e+02	3.15e+02	2.71e-01	6.00e-01	Bare_Uranium_Spheres.ult
H	Probability vs Rho-R (Energy = 10^-6)	1.95e+02	3.15e+02	3.30e-01	7.11e-01	Bare_Uranium_Spheres.ult
I	Probability vs Rho-R (Energy = 10^-7)	1.95e+02	3.15e+02	3.24e-01	6.90e-01	Bare_Uranium_Spheres.ult

(b)

Figure 3. **Mercury** predictions of the single-particle initiation probabilities for the modified bare uranium sphere test problems as a function of (a) source energy and (b) optical depth ρr.

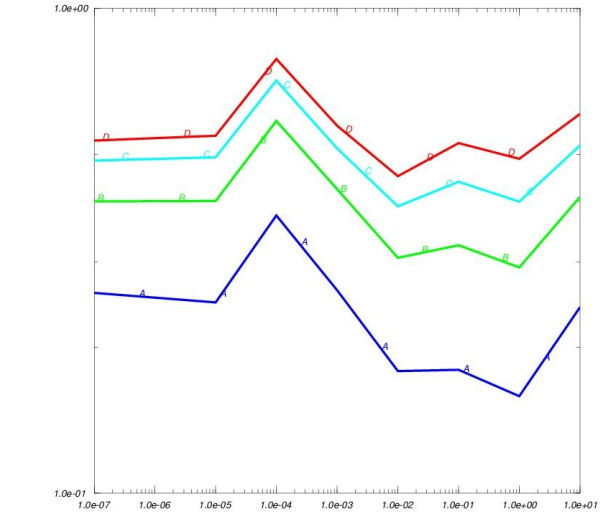

CURVE	LABEL	XMIN	XMAX	YMIN	YMAX	FILE
A	Probability vs Energy (Rho-R = 120)	1.00e-07	1.00e+01	1.59e-01	3.74e-01	Bare_Plutonium_Spheres.ult
B	Probability vs Energy (Rho-R = 140)	1.00e-07	1.00e+01	2.92e-01	5.86e-01	Bare_Plutonium_Spheres.ult
C	Probability vs Energy (Rho-R = 160)	1.00e-07	1.00e+01	3.91e-01	7.10e-01	Bare_Plutonium_Spheres.ult
D	Probability vs Energy (Rho-R = 180)	1.00e-07	1.00e+01	4.51e-01	7.87e-01	Bare_Plutonium_Spheres.ult

(a)

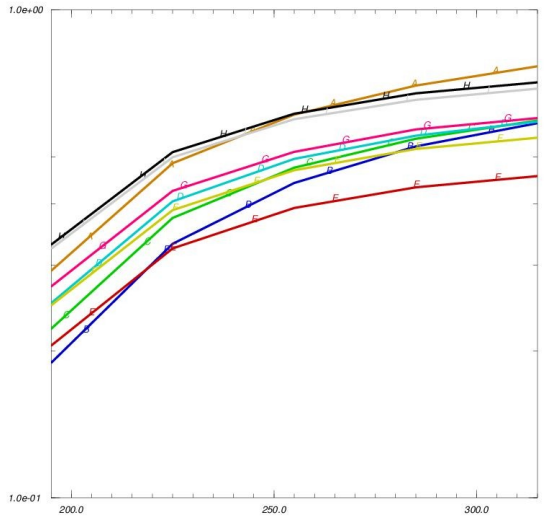

CURVE	LABEL	XMIN	XMAX	YMIN	YMAX	FILE
A	Probability vs Rho-R (Energy = 10^+1)	1.95e+02	3.15e+02	2.92e-01	7.66e-01	Bare_Uranium_Spheres.ult
B	Probability vs Rho-R (Energy = 10^+0)	1.95e+02	3.15e+02	1.89e-01	5.86e-01	Bare_Uranium_Spheres.ult
C	Probability vs Rho-R (Energy = 10^-1)	1.95e+02	3.15e+02	2.22e-01	5.93e-01	Bare_Uranium_Spheres.ult
D	Probability vs Rho-R (Energy = 10^-2)	1.95e+02	3.15e+02	2.50e-01	5.90e-01	Bare_Uranium_Spheres.ult
E	Probability vs Rho-R (Energy = 10^-3)	1.95e+02	3.15e+02	2.05e-01	4.57e-01	Bare_Uranium_Spheres.ult
F	Probability vs Rho-R (Energy = 10^-4)	1.95e+02	3.15e+02	2.48e-01	5.47e-01	Bare_Uranium_Spheres.ult
G	Probability vs Rho-R (Energy = 10^-5)	1.95e+02	3.15e+02	2.71e-01	6.00e-01	Bare_Uranium_Spheres.ult
H	Probability vs Rho-R (Energy = 10^-6)	1.95e+02	3.15e+02	3.30e-01	7.11e-01	Bare_Uranium_Spheres.ult
I	Probability vs Rho-R (Energy = 10^-7)	1.95e+02	3.15e+02	3.24e-01	6.90e-01	Bare_Uranium_Spheres.ult

(b)

Figure 4. **Mercury** predictions of the single-particle initiation probabilities for the modified bare plutonium sphere test problems as a function of (a) source energy and (b) optical depth ρr.

The initiation probabilities $p(r,E,t)$ predicted by **Mercury** are shown in Figures 3 and 4 for the modified suite of uranium and plutonium bare-sphere test problems, respectively. Figures 3a and 4a present the results for the various values of ρr as a function of source energy, while Figures 3b and 4b present the results for the various values of source energy as a function of ρr. In the interest of brevity, the results from these $\mathcal{O}(100)$ calculations are not tabulated here, but this data may be obtained from the authors by contacting at the e-mail addresses listed above. These results were obtained with the same model parameters and cross sections as described above. The monoenergetic sources produce the same increase in $p(r,E,t)$ with increasing ρr that was observed for the fission-spectrum energy dependence of the source. The variation of $p(r,E,t)$ with source energy is non-monotonic and quite complex. The peaks and troughs in Figures 3a and 4a are generally *not* correlated with the energy variation of the total, fission or capture cross sections. These cross sections tend to decrease by several orders of magnitude with increasing neutron energies in the range $10^{-7} < E < 10^{-1}$ MeV, and are reasonably constant for $E > 10^{-1}$ MeV. Of course, leakage also plays an important role in terminating fission chains through the loss of individual neutron progeny. Since high energy neutrons are more likely to escape from the system than low energy neutrons (due to larger velocities), one might conclude that the probability of initiation might fall off with increasing neutron energy. However, this is not borne out by the results shown in Figure 3a and 4a.

4. SUMMARY, CONCLUSIONS AND FUTURE WORK

A probability of initiation method has been developed in the **Mercury** Monte Carlo code. This new method represents an analog solution of the standard form of the Boltzmann transport equation, in contrast to many deterministic codes which iteratively solve the non-linear, adjoint form of the equation. This new method uses a modified version of time-dependent source calculation technique. The user specifies the spatial- and energy-dependence of a source, from which neutrons are injected into the system. These (C_i) neutrons form the progenitors of a series of neutron families or chains. The neutron chains are then tracked for a user-specified maximum period of time (max_age). The number of progeny in each chain is periodically tallied, and the chain is successfully terminated when the size of the family exceeds a user-specified threshold for a self-sustaining, or divergent, chain (successful_chain_ threshold). The initiation probability is defined as the ratio of the number of divergent chains (C_d) to the number of initial chains $p \equiv C_d / C_i$.

The user of the new method needs to choose the model parameters judiciously, in an attempt to balance the accuracy and efficiency of the calculation. The threshold for a divergent chain should be set in the range 1000 < successful_chain_threshold < 10000. In addition, max_age should be set large enough to ensure converged, asymptotic results, while at the same time being set short enough to avoid violating the assumption of a static system, which is an inherent feature of the initiation probability equation.

This new method has been applied to an existing suite of probability of initiation test problems, and the results have been compared with those from three deterministic transport codes. The agreement between the deterministic and Monte Carlo results is rather good, especially since these codes used different numerical techniques and nuclear data. In an effort to eliminate the ambiguity of the source definition on the calculated initiation probability, we have developed a

modified suite of test problems for use by the community, and have provided results from **Mercury** for comparison.

In the future, we intend to validate this new method against experiment data from pulsed reactors. This method will be used to calculate the initiation probability and burst wait time in the Caliban and Godiva-II systems. In an effort to determine the impact of nuclear data on the calculated probabilities, the suites of test problems described above will be recalculated using different evaluated nuclear data bases. Recent work by the nuclear data team at LLNL has provided our transport codes with the ability to use ENDF-B/VI, ENDF-B/VII and JEF-3 data. These data bases will be used to determine whether the observed discrepancies between the **Mercury** and **Partisn** results arise from the use of different algorithms or nuclear data.

ACKNOWLEDGMENTS

The authors wish to acknowledge helpful discussions with several individuals, including Randy Baker (LANL), Jim Ferguson (LLNL) and Peter Brown (LLNL). We are indebted to Randy and Peter for providing us with the results from their calculations of the probability of initiation test problems. This work was performed under the auspices of the U. S. Department of Energy by the University of California, Lawrence Livermore National Laboratory (LLNL) under Contract W-7405-Eng-48.

REFERENCES

1. G. I. Bell, "On the Stochastic Theory of Neutron Transport", *Nucl. Sci. Eng.*, **21**, pp. 390 - 401 (1965).

2. R. J. Procassini and M. S. McKinley (editors), "The Mercury Monte Carlo Code Web Site", Lawrence Livermore National Laboratory, Web Document UCRL-WEB-212708, http://www.llnl.gov/Mercury (2005).

3. R. J. Procassini, J. M. Taylor, M. S. McKinley, G. M. Greenman, D. E. Cullen, M. J. O'Brien, B. R. Beck and C. A. Hagmann, "Update on the Development and Validation of Mercury: A Modern, Monte Carlo Particle Transport Code", in *Proceedings of the International Topical Meeting on Mathematics and Computation, Supercomputing, Reactor Physics and Nuclear and Biological Applications*, 12 - 15 September 2005, Avignon, France (2005).

4. R. E. Alcouffe, R. S. Baker, S. A. Turner and J. A. Dahl, "PARTISN: A Time-Dependent, Parallel Neutral Particle Transport Code System", Los Alamos National Laboratory, Report LA-UR-02-5633 (2002).

5. U. Hannebutte and P. N. Brown, "Ardra: Scalable Parallel Code System to Perform Neutron and Radiation Transport Calculations", Lawrence Livermore National Laboratory, Report UCRL-TB-132078 (1999).

6. C. J. Clouse, "Parallel Deterministic Neutron Transport with AMR", in *Computational Methods in Transport*, edited by F.R. Graziani, Springer-Verlag, pp. 499 - 512 (2006).

7. J. M. Ferguson, Private communication (2004).

8. D. P. McNabb and M. S. McKinley (editors), "Computational Nuclear Physics: ENDL Overview", Lawrence Livermore National Laboratory, Web Document UCRL-WEB-200195, http://nuclear.llnl.gov/CNP/ENDL (2003).

9. G. D. Spriggs, "Evaluation of MENDF5 and MENDF6 Using Measured Integral Parameters in Godiva-I and Jezebel", Los Alamos National Laboratory, Report LA-UR-02-1809 (2002).

10. J. Terrell, "Distributions of Fission Neutron Numbers", *Phys. Rev.*, **108**, pp. 783-789 (1957).